HHS Public Access

Author manuscript

Cell Rep. Author manuscript; available in PMC 2021 May 10.

Published in final edited form as:

Cell Rep. 2021 March 30; 34(13): 108921. doi:10.1016/j.celrep.2021.108921.

SIRT2 promotes BRCA1-BARD1 heterodimerization through deacetylation

Elizabeth V. Minten[1], **Priya Kapoor-Vazirani**[1], **Chunyang Li**[1], **Hui Zhang**[1], **Kamakshi Balakrishnan**[1], **David S. Yu**[1,2,*]

[1]Department of Radiation Oncology and Winship Cancer Institute, Emory University School of Medicine, Atlanta, GA 30322, USA

[2]Lead contact

SUMMARY

The breast cancer type I susceptibility protein (BRCA1) and BRCA1-associated RING domain protein I (BARD1) heterodimer promote genome integrity through pleiotropic functions, including DNA double-strand break (DSB) repair by homologous recombination (HR). BRCA1-BARD1 heterodimerization is required for their mutual stability, HR function, and role in tumor suppression; however, the upstream signaling events governing BRCA1-BARD1 heterodimerization are unclear. Here, we show that SIRT2, a sirtuin deacetylase and breast tumor suppressor, promotes BRCA1-BARD1 heterodimerization through deacetylation. SIRT2 complexes with BRCA1-BARD1 and deacetylates conserved lysines in the BARD1 RING domain, interfacing BRCA1, which promotes BRCA1-BARD1 heterodimerization and consequently BRCA1-BARD1 stability, nuclear retention, and localization to DNA damage sites, thus contributing to efficient HR. Our findings define a mechanism for regulation of BRCA1-BARD1 heterodimerization through SIRT2 deacetylation, elucidating a critical upstream signaling event directing BRCA1-BARD1 heterodimerization, which facilitates HR and tumor suppression, and delineating a role for SIRT2 in directing DSB repair by HR.

In brief

Minten et al. show that SIRT2, a sirtuin deacetylase and tumor suppressor protein, promotes BRCA1-BARD1 heterodimerization through deacetylation of BARD1 at conserved lysines within

*Correspondence: dsyu@emory.edu.

AUTHOR CONTRIBUTIONS

E.V.M., C.L., H.Z., and D.S.Y. conceived and designed the study. E.V.M., P.K.-V., C.L., and K.B. performed the experiments. E.V.M. and D.S.Y. wrote the manuscript with input from all authors.

SUPPLEMENTAL INFORMATION

Supplemental information can be found online at https://doi.org/10.1016/j.celrep.2021.108921.

DECLARATION OF INTERESTS

The authors declare no competing interests.

INCLUSION AND DIVERSITY

While citing references scientifically relevant for this work, we also actively worked to promote gender balance in our reference list. The author list of this paper includes contributors from the location where the research was conducted who participated in the data collection, design, analysis, and/or interpretation of the work.

its RING domain. These findings elucidate a critical upstream signaling event directing BRCA1-BARD1 heterodimerization, which facilitates HR and tumor suppression.

Graphical Abstract

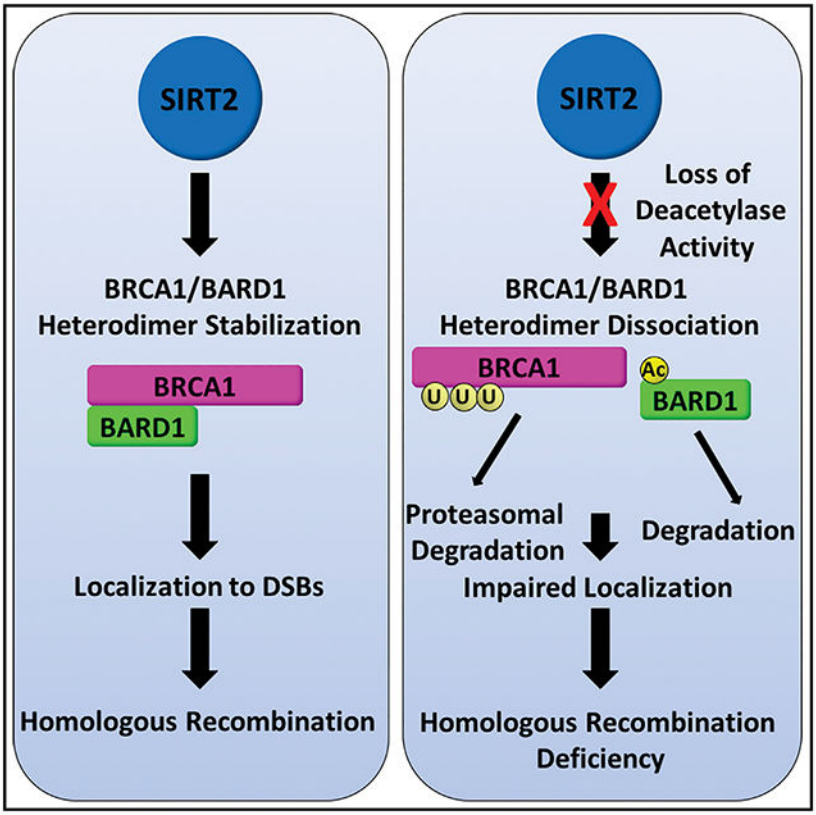

INTRODUCTION

Inherited mutations in *BRCA1* predispose to breast and ovarian cancers (Foulkes, 2008; Roy et al., 2011; Silver and Livingston, 2012; Tarsounas and Sung, 2020; Venkitaraman, 2014). BRCA1 promotes genome integrity through pleiotropic functions, including double-strand break (DSB) repair by homologous recombination (HR) (Moynahan et al., 1999, 2001; Scully et al., 1997; Snouwaert et al., 1999), protection of stalled replication forks from nucleolytic degradation (Schlacher et al., 2012), cell cycle checkpoint activation (Xu et al., 1999, 2001; Yarden et al., 2002), mRNA splicing and microRNA biogenesis (Chang and Sharan, 2012; Kawai and Amano, 2012; Kleiman and Manley, 1999; Kleiman and Manley, 2001; Savage et al., 2014), and avoidance of replication-transcription conflicts (Hatchi et al., 2015; Schlacher et al., 2012). In particular, BRCA1's role in multiple steps in the error-free HR pathway, which helps repair DSBs and resolve stalled replication forks, is thought to be important for its tumor suppressor function (Irminger-Finger and Jefford, 2006; Jiang and Greenberg, 2015; Kolinjivadi et al., 2017; Moynahan and Jasin, 2010; Tarsounas and Sung, 2020).

BRCA1 forms a stable heterodimeric complex with BARD1 through the association of their amino (N)-terminal RING domains (Meza et al., 1999; Wu et al., 1996), which is important for their mutual stability (Hashizume et al., 2001; Joukov et al., 2001), nuclear localization (Fabbro et al., 2002; Rodriguez et al., 2004), recruitment to DNA damage sites (Fabbro et al., 2002; Rodriguez et al., 2004), and ubiquitin E3 ligase activity (Hashizume et al., 2001; Mallery et al., 2002; Ruffner et al., 2001; Xia et al., 2003). Mice deficient in *Brca1* or *Bard1* develop indistinguishable basal-like mammary carcinomas (Shakya et al., 2008), suggesting that the tumor suppressor functions of BRCA1 and BARD1 are likely mediated through their heterodimerization. Indeed, the RING domain of BRCA1 is essential for tumor suppression in a conditional mouse model for *BRCA1*-associated breast cancer carrying *C61G*, a common pathogenic missense variant that disrupts BRCA1-BARD1 heterodimerization (Drost et al., 2011). Furthermore, a number of additional germline mutations in the RING domains of *BRCA1* and *BARD1* have been found in patients with hereditary breast and ovarian cancers (Database: BRCA Exchange) (Brzovic et al., 2001a; Castilla et al., 1994; Friedman et al., 1994; Ruffner et al., 2001), highlighting the potential significance of BRCA1-BARD1 heterodimerization in tumor suppression. Mutational analyses based on the nuclear magnetic resonance (NMR) structure of the BRCA1-BARD1 RING domain heterodimer complex, which consists of a pair of RING finger motifs and flanking anti-parallel α helices (which we will henceforth refer to as the RING domain) (Brzovic et al., 2001b), have shown that the BRCA1-BARD1 interface is mediated by residues important for hydrophobic interactions or that contribute to structural stabilization (Brzovic et al., 2003; Lee et al., 2015; Meza et al., 1999; Morris et al., 2002; Xia et al., 2003); however, although suggested, the contribution of charged interactions has not been demonstrated (Brzovic et al., 2001b).

The interaction of BRCA1 and BARD1 is critical for their mutual stability (Hashizume et al., 2001; Joukov et al., 2001), likely by masking BRCA1's degron domain, which is located in its first 167 amino acids (Lu et al., 2007), and is ubiquitinated by HERC2 (Wu et al., 2010), HUWE1 (Wang et al., 2014), and FBXO44 (Lu et al., 2012) and deubiquitinated by USP9X (Lu et al., 2019). CTSS, a cysteine protease, has also been shown to promote BRCA1 ubiquitination and subsequent degradation after cleaving its C-terminal BRCT domains (Kim et al., 2019). BARD1 is also degraded in a ubiquitination-mediated process via the APC/C complex (Song and Rape, 2010). Furthermore, BRCA1-BARD1 stability is affected by their interaction with UBE2T (Ueki et al., 2009), GUARDIN (Hu et al., 2018), TACC3 (Kim et al., 2018), and TUSC4 (Peng et al., 2015), suggesting tight regulation of BRCA1-BARD1 stability.

Sirtuin 2 (SIRT2) is a sirtuin family NAD^+-dependent deacetylase, which regulates multiple biological processes, including genome maintenance, aging, tumorigenesis, and metabolism (Finkel et al., 2009; Guarente, 2011; Saunders and Verdin, 2007; Zhang et al., 2016b). Significantly, mice deficient in *Sirt2* develop breast and other cancers (Kim et al., 2011; Serrano et al., 2013), suggesting that SIRT2 functions in tumor suppression. We previously defined a role for SIRT2 in directing the replication stress response (RSR), a subset of the DNA damage response (DDR), through the acetylation status of ATRIP and CDK9 (Zhang et al., 2013, 2016a, 2016b) and furthermore showed that somatic cancer-associated *SIRT2* mutations impair the activity of SIRT2 in maintaining genome integrity (Head et al., 2017);

however, SIRT2's role in downstream DNA repair is less well established. SIRT2 was recently reported to promote nucleotide excision repair (NER) (Zhang et al., 2020), but its role in promoting DSB repair by HR is unclear. Furthermore, BRCA1 function in the intra-S checkpoint is activated by K830 acetylation via a pCAF/SIRT1 axis (Lahusen et al., 2018); however, the role of SIRT2 deacetylation, or more generally of upstream signaling events, in governing BRCA1-BARD1 heterodimerization is not known.

In this study, we show that BARD1 deacetylation by SIRT2 at conserved lysine sites in its RING domain promotes BRCA1-BARD1 heterodimerization, thereby facilitating BRCA1-BARD1 stability, nuclear retention, localization to DNA damage sites, and function in HR. Our findings define a mechanism for regulation of BRCA1-BARD1 heterodimerization through SIRT2 deacetylation, elucidating a critical upstream signaling event directing BRCA1-BARD1 heterodimerization and delineating a role for SIRT2 in promoting DSB repair by HR.

RESULTS

SIRT2 interacts with the BRCA1-BARD1 complex

To determine if SIRT2 interacts in a complex with BRCA1 and BARD1, we performed co-immunoprecipitation (coIP) analyses. coIP of SIRT2-FLAG expressed in human embryonic kidney (HEK) 293T cells pulled down HA-BRCA1 and endogenous BARD1 (Figure 1A). In a reciprocal coIP, HA-BRCA1 pulled down GFP-SIRT2 and endogenous BARD1, and endogenous BARD1 pulled down SIRT2-FLAG and endogenous BRCA1 (Figures 1B and 1C). The endogenous interaction of SIRT2 with BRCA1 and BARD1 was validated by coIP in HeLa cervical and HCT116 colorectal cancer cells (Figures 1D and 1E). Furthermore, the coIP of HA-BRCA1 with SIRT2-FLAG and endogenous BARD1 in HEK293T cells was preserved even following treatment with ethidium bromide, an intercalating agent, which disrupts protein-DNA interactions (Figure S1A). Thus, the interaction of SIRT2 with BRCA1 and BARD1 is physiologic, not cell type specific, and not mediated through DNA.

SIRT2 deacetylates BRCA1 and BARD1

To determine if SIRT2 deacetylates BRCA1, we performed an *in vitro* deacetylation assay with purified acetylated HA-BRCA1, SIRT2-FLAG, and NAD^+ with or without nicotinamide, a sirtuin inhibitor. SIRT2-FLAG wild-type (WT) but not H187Y, a deacetylase-inactive mutant (North et al., 2003), deacetylated HA-BRCA1 in an NAD^+-dependent manner, in which deacetylation was inhibited by nicotinamide (Figures 1F and S1B). These findings were validated in HEK293T cells, in which SIRT2-FLAG WT but not H187Y deacetylated HA-BRCA1 (Figure 1G). Similar results were obtained for BARD1, in which SIRT2-FLAG WT but not H187Y deacetylated acetylated GFP-BARD1 *in vitro* in a NAD^+-dependent manner that was inhibited by nicotinamide (Figure 1H), and SIRT2-FLAG deacetylated GFP-BARD1 expressed in HEK293T cells (Figure 4F).

SIRT2 deacetylase activity promotes BRCA1-BARD1 stability

To determine the functional significance of this interaction, BRCA1 protein levels were measured by western blot analysis in HCT116 cells after SIRT2 knockdown. BRCA1 levels

were decreased following SIRT2 knockdown (Figure 2A), which was also observed in U2OS cells (Figures S2A–S2B). As BRCA1 and BARD1 stabilize each other when in complex (Hashizume et al., 2001; Joukov et al., 2001), decreased BARD1 levels were also reduced after SIRT2 knockdown (Figures 2B and S2A). Treatment with AGK2, a SIRT2-specific inhibitor (Outeiro et al., 2007), produced similar results, indicating that these results were dependent on SIRT2 deacetylase activity (Figures 2D and 2E). To determine if SIRT2 regulates BRCA1 and BARD1 at the transcriptional level, we performed quantitative RT-PCR following SIRT2 depletion or AGK2 treatment. No corresponding significant decrease in BRCA1 or BARD1 mRNA levels was observed (Figures 2C and 2F), suggesting that regulation occurs at the post-transcriptional level. To validate these findings, HEK293T cells were treated with cycloheximide, an inhibitor of translation, alone or with AGK2. A significantly greater decrease in BRCA1 protein levels was observed following AGK2 treatment (Figures 2G and 2H). We observed no significant difference in BARD1 protein levels at this time point, consistent with prior reports of BARD1's significantly longer half-life (Choudhury et al., 2004), and combined AGK2 and cycloheximide treatment times beyond the 8 h required to detect noticeable BARD1 degradation (Choudhury et al., 2004) resulted in significant toxicity (data not shown). The decrease in BRCA1 and BARD1 protein levels following SIRT2 knockdown or AGK2 treatment was alleviated by proteasomal inhibition with MG132 (Figures 2I, 2J, and S2C), suggesting that SIRT2 deacetylase activity promotes BRCA1-BARD1 stability by impairing its degradation. The decrease in BRCA1 protein levels following SIRT2 knockdown was also observed in cells synchronized in G1, S, and G2/M phase (Figures S2D and S2E), implying a cell cycle-independent effect, while a decrease in BARD1 protein levels following SIRT2 knockdown was observed in cells synchronized in G1 and to a lesser extent in G2/M but not S phase, which may be due to BARD1's maximal mRNA expression in S phase and longer half-life (Choudhury et al., 2004). Moreover, SIRT2 knockdown and AGK2 treatment caused a significant decrease in BRCA1 and BARD1 protein levels in both the absence and presence of ionizing radiation (IR) (Figures S2F–S2J). Collectively, our data suggest that SIRT2 deacetylase activity promotes BRCA1-BARD1 stability by impairing its degradation independent of cell cycle and DNA damage.

SIRT2 deacetylase activity promotes BRCA1-BARD1 nuclear retention, localization to DNA damage sites, and HR

The BRCA1-BARD1 interaction has been reported to mask each other's nuclear export signals (NESs), thereby promoting their nuclear retention (Fabbro et al., 2002; Rodriguez et al., 2004). We thus hypothesized that SIRT2 deficiency might result in increased cytoplasmic localization. Indeed, a significantly greater increase in BRCA1 and BARD1 cytoplasmic localization was observed in U2OS cells depleted for SIRT2 or treated with AGK2 (Figures 3A–3F). To determine if SIRT2 deficiency furthermore impairs BRCA1-BARD1 localization to DNA damage sites, we examined U2OS cells treated with IR following SIRT2 depletion. A significantly greater decrease in cells with IR-induced BRCA1 and BARD1 foci co-localizing with γH2AX foci was observed following SIRT2 deficiency (Figures 3G–3J). Moreover, SIRT2 deficiency impaired the co-localization of BRCA1 and BARD1 with mCherry-LacI-FokI endonuclease-induced DSBs in U2OS reporter cells integrated with lac operator repeats (Shanbhag et al., 2010) (Figures S3A and

S3B), suggesting that SIRT2 promotes BRCA1-BARD1 localization to DNA damage sites and that SIRT2 may direct BRCA1-BARD1 function in DSB repair. To determine directly if SIRT2 functions in HR, we examined SIRT2 depletion in U2OS cells integrated with a direct repeat (DR)-GFP reporter substrate in which expression of the I-SceI endonuclease generates a DSB that when repaired by HR restores GFP expression. SIRT2 depletion caused a significant impairment in HR, which could be rescued by SIRT2-FLAG WT but not H187Y (Figures 3K, 3L, and S3C). Moreover, in epistasis studies, combined SIRT2 and BRCA1 depletion caused no significant further impairment in HR compared with BRCA1 depletion alone (Figures 3M, 3N, and S3D), implying that SIRT2 functions with BRCA1 in promoting HR. Interestingly, BRCA1 knockdown also caused an increase in SIRT2 protein levels (Figure 3N), suggesting that BRCA1 may be involved in a feedback loop to regulate SIRT2. Collectively, our results suggest that SIRT2 deacetylation promotes BRCA1-BARD1 nuclear retention and localization to DNA damage sites, and thus facilitating HR.

SIRT2 deacetylates the BARD1 RING domain

The stability and nuclear retention of BRCA1-BARD1 is dependent on heterodimerization of its RING motifs and flanking α helices (RING domain) located in their respective N-termini (Fabbro et al., 2002; Hashizume et al., 2001; Joukov et al., 2001). Moreover, the BRCA1 degron has also been mapped to its N terminus (Lu et al., 2007). To provide insight into the mechanism by which SIRT2 may regulate BRCA1-BARD1 stability, we mapped the regions of BRCA1 and BARD1 interacting with SIRT2. coIP of overlapping FLAG-HA-NLS BRCA1 fragments (Lu et al., 2007) spanning full-length (FL) BRCA1 and GFP-SIRT2 expressed in HEK293T cells revealed that FLAG-HA-NLS BRCA1 (1–324) but not BRCA1 (263–551) or more C-terminal BRCA1 interacts with GFP-SIRT2 (Figure 4A). In further mapping experiments, His-SIRT2 co-immunoprecipitated with BRCA1 (1–167) (Figure S4A), suggesting that BRCA1 amino acids 1–167, where its degron is located, are sufficient for interaction with SIRT2. Interestingly, the BARD1-binding domain is also located in this region (Wu et al., 1996), and BARD1 has been reported to stabilize BRCA1 by protecting it from ubiquitination (Choudhury et al., 2004). Indeed, a FLAG-BARD1 fragment containing residues 1–202 but not a deletion mutant missing residues 34–126 (Laufer et al., 2007), corresponding to BARD1's RING domain, co-immunoprecipitated with GFP-SIRT2 (Figure 4B), suggesting that BARD1 amino acids 34–126 are necessary and 1–202 are sufficient for interaction with SIRT2. Moreover, HA-BRCA1 C61G, a pathogenic mutant with impaired ability to bind BARD1 (Brzovic et al., 1998), failed to pull down SIRT2-FLAG (Figure 4C), suggesting that BRCA1 interacts with SIRT2 through its interaction with BARD1. Collectively, these findings imply that SIRT2 interacts with the BRCA1-BARD1 complex through BARD1's N-terminal RING domain.

To identify the specific lysine targets of SIRT2 deacetylation, we analyzed the NMR structure of the BRCA1-BARD1 heterodimer complex (Brzovic et al., 2001b) (Figures 4D and S4B). Of note, the positive charge of BARD1 lysine 96 (K96) forms a potential salt bridge with the negative charge of BRCA1 aspartic acid 40 (D40) measuring 2.2 Å, and to a lesser extent, potential electrostatic interactions measuring about 5 Å are formed between BARD1 K46 and BRCA1 glutamic acid 85 (E85) and BARD1 K100 and BRCA1 E10. All three BARD1 lysine sites are evolutionarily conserved (Figure S4C), and acetylation at these

sites may lead to a loss of electrostatic attraction with the corresponding negative charged residue on BRCA1. Although HA-BRCA1 is acetylated (Figure S4D), we found no evidence that BRCA1 is acetylated at its N terminus (1–167), which contains its RING domain, by IP of FLAG-HA-NLS BRCA1 (1–167) and western blot with an anti-acetyl K antibody (Figure S4E) or reciprocally, IP with an anti-acetyl K antibody and western blot for FLAG-HA-NLS BRCA1 (1–167) (Figure S4F). In contrast, GFP-BARD1 is acetylated, and mutation of BARD1 K46, K96, and K110 to arginines (3KR) caused a significant decrease in acetylation of BARD1 (Figure 4E). Mass spectrometry of purified GFP-BARD1 from cells identified additional candidate acetylation sites outside of the BARD1 RING domain at K130, K596, K630, and K593, although only GFP-BARD1 K596R showed a decrease in acetylation compared with GFP-BARD1 WT (Figure 4E). However, overexpression of SIRT2-FLAG caused a significant decrease in acetylation of GFP-BARD1 WT and K596R but not 3KR (Figure 4F), suggesting that SIRT2 primarily deacetylates BARD1 at its RING motif and flanking α helices among K46, K96, and K110 but not at K596R.

BARD1 RING domain deacetylation by SIRT2 promotes BRCA1-BARD1 heterodimerization

To determine whether SIRT2 regulates the interaction of BRCA1 and BARD1, we performed coIP of GFP-BARD1 in HEK293T cells treated with a short course of AGK2 to minimize significant degradation of BRCA1 and BARD1 and found that GFP-BARD1 pulled down a lower amount of endogenous BRCA1 following AGK2 treatment than a control (Figure 5A). Similarly, a reciprocal coIP of HA-BRCA1 pulled down a decreased amount of GFP-BARD1 following AGK2 treatment (Figures 5B and S5A). Moreover, AGK2 treatment impaired the coIP of endogenous BARD1 and endogenous BRCA1 (Figures S5B and S5C), suggesting that SIRT2 deacetylase activity promotes the interaction of BRCA1 and BARD1.

We then analyzed the interaction of endogenous BRCA1 with GFP-BARD1 WT, 3KR, or a mutant in which K46, K96, and K110 were replaced by glutamine (Q) to mimic an acetylated state (3KQ). Strikingly, coIP of GFP-BARD1 3KR pulled down a significantly greater amount of endogenous BRCA1 than GFP-BARD1 WT (Figures 5C and S5D), while coIP of GFP-BARD 3KQ pulled down a significantly decreased amount of endogenous BRCA1 compared with GFP-BARD1 WT (Figures 5D and S5D), suggesting that BARD1 acetylation at its RING domain impairs interaction with BRCA1. In contrast, coIP of GFP-BARD1 K596R mutant pulled down a comparable amount of endogenous BRCA1 as GFP-BARD1 WT (Figure S5E), and coIP of FL HA-BRCA1 in which all 14 lysines within amino acids 1–167 that complex with SIRT2 were mutated to arginine (14KR) pulled down a comparable amount of GFP-BARD1 WT as HA-BRCA1 WT (Figure S5F). We next examined BRCA1 protein levels in HEK293T cells expressing GFP-BARD1 WT or GFP-BARD1 3KR and treated with or without cycloheximide and AGK2. Four hours after cycloheximide treatment, a greater amount of endogenous BRCA1 was observed in cells expressing GFP-BARD1 3KR compared with WT (Figures 5E and 5F). Moreover, expression of GFP-BARD1 3KR rescued the degradation of BRCA1 caused by AGK2 treatment (Figures 5G and 5H), implying that SIRT2 deacetylation of the BARD1 RING domain promotes BRCA1 stability. The decrease in coIP between GFP-BARD1 and endogenous BRCA1 following SIRT2 depletion was also rescued by expression of GFP-

BARD1 3KR compared with WT (Figure 5I), demonstrating unequivocally that SIRT2 promotes the interaction of BRCA1 and BARD1 through deacetylation of its RING domain. Furthermore, we observed a decreased amount of BRCA1 foci co-localizing with FokI-induced DSBs when normalized to GFP-BARD1 foci fluorescence following SIRT2 knockdown, with expression of GFP-BARD1 3KQ compared with WT and 3KR (Figure S5G), implying that BARD1 RING domain deacetylation by SIRT2 contributes, at least in part, to BRCA1 localization to DNA damage sites. Significantly, overexpression of RFP-BARD1 WT and 3KR but not 3KQ restored the HR impairment of SIRT2 depletion to near control levels (Figures 5J, 5K, and S5H). Moreover, expression of GFP-BARD1 3KR and to a lesser extent WT but not 3KQ alleviated the impairment in co-localization of RAD51 to mCherry-LacI-FokI endonuclease-induced DSBs of SIRT2 deficiency (Figures S5I–S5K). Collectively, these data demonstrate that BARD1 functions downstream of SIRT2 in promoting HR and show unequivocally that SIRT2 promotes HR through deacetylation of BARD1 at its RING domain within K46, K96, and K110.

DISCUSSION

Our findings reveal a critical upstream regulatory mechanism governing BRCA1-BARD1 heterodimerization through SIRT2 deacetylation and provide important insights into the interplay between the SIRT2 and BRCA1-BARD1 breast tumor suppressor proteins, whereby BARD1 deacetylation by SIRT2 at conserved lysine sites in its RING domain, critical for interfacing with BRCA1 through charged interactions, promotes BRCA1-BARD1 heterodimerization, thereby facilitating their mutual stability, nuclear retention, localization to DNA damage sites, and function in HR. Furthermore, these findings identify BRCA1-BARD1 as an interacting partner and substrate for SIRT2, establish SIRT2 as a positive regulator of DSB repair by HR, and further our understanding of how *Sirt2* deficiency results in genomic instability and carcinogenesis.

BRCA1-BARD1 heterodimerization is critical for its functions in HR and tumor suppression (Jiang and Greenberg, 2015; Kolinjivadi et al., 2017; Moynahan and Jasin, 2010; Tarsounas and Sung, 2020). Indeed, a number of germline mutations in the RING domains of *BRCA1* and *BARD1* have been found in patients with hereditary breast and ovarian cancers (Drost et al., 2011). Previous mutational analyses have reported that the BRCA1-BARD1 interface is mediated by residues important for hydrophobic interactions or that contribute to structural stabilization (Brzovic et al., 2003; Lee et al., 2015; Meza et al., 1999; Morris et al., 2002; Xia et al., 2003). Given that BARD1 3KR has increased interactions with BRCA1 and BARD1 3KQ has impaired interactions with BRCA1, our data support a model whereby BARD1 acetylation at its RING domain (K46, K96, and/or K110) leads to loss of electrostatic interaction with the corresponding negatively charged residues in BRCA1, thereby impairing BRCA1-BARD1 heterodimerization (Figure 5L). This leads to increased access to the BRCA1 N-terminal degron for ubiquitination and proteasomal degradation, which in turn destabilizes BARD1. Impairment of BRCA1-BARD1 heterodimerization also leads to unmasking of the BRCA1 and BARD1 NESs, leading to cytoplasmic accumulation, impaired localization to DNA damage sites, and impaired HR. BARD1 deacetylation by SIRT2 at its RING domain promotes charged interactions leading to BRCA1-BARD1

heterodimerization, thereby facilitating BRCA1-BARD1 stability, nuclear retention, localization to DNA damage sites, and function in HR.

Given that SIRT2 deficiency and BARD1 3KQ does not fully abolish interaction with BRCA1, it is likely that there are additional mechanisms contributing to BRCA1-BARD1 heterodimerization. Although we have found that SIRT2 deacetylates BRCA1 *in vitro* and in cells, we have found no evidence that the N terminus of BRCA1 is acetylated and furthermore showed that a BRCA1 N-terminal 14KR mutant does not facilitate heterodimerization with BARD1. Moreover, as BARD1 3KR can rescue the heterodimerization impairment of SIRT2 deficiency, the functional significance of BRCA1 deacetylation by SIRT2 is likely not related to BRCA1-BARD1 heterodimerization. In addition, it is possible that other factors, such as GUARDIN (Hu et al., 2018) and TACC3 (Kim et al., 2018), may also contribute to BRCA1-BARD1 heterodimerization; however, their precise mechanisms have not yet been fully elucidated. Although our data suggest that SIRT2 deacetylation of the BARD1 RING domain facilitates BRCA1 localization to DNA damage sites, as we observed a decreased amount of BRCA1 foci co-localizing with FokI-induced DSBs when normalized to GFP-BARD1 foci fluorescence following SIRT2 knockdown with expression of GFP-BARD1 3KQ compared with WT and 3KR, our model does not exclude the possibility of BRCA1-BARD1 degradation also contributing to impaired localization. Finally, it is interesting that expression of GFP-BARD1 WT can rescue the HR impairment but not degradation or heterodimerization impairment of SIRT2 depletion or inhibition. It is possible that when GFP-BARD1 WT is overexpressed, there is still sufficient albeit less BRCA1-BARD1 heterodimers to rescue HR.

We have previously shown that SIRT2 directs the RSR at least in part through deacetylation of ATRIP and CDK9 (Zhang et al., 2013, 2016a). Our finding that SIRT2 promotes DSB by HR provides further evidence that SIRT2 also has a role in downstream DNA repair in addition to its previously defined function in upstream checkpoint signaling. Furthermore, the identification of BARD1 as a binding partner and substrate of SIRT2 adds to the growing number of SIRT2 substrates that function in promoting genome integrity, providing support for SIRT2 in regulating a network of proteins involved in the DDR (Zhang et al., 2016b). Our finding that SIRT2 directs BRCA1-BARD1 function in HR provides an additional layer of insight into how SIRT2 dysregulation leads to genomic instability and carcinogenesis. In this regard, it is noteworthy that similar to BRCA1 and BARD1, SIRT2 also functions in breast tumor suppression (Kim et al., 2011; Serrano et al., 2013). Dissecting BRCA1-BARD1's precise contributions to SIRT2's breast tumor suppressor function will be of significant future clinical interest.

STAR★METHODS

RESOURCE AVAILABILITY

Lead contact—Further information and requests for resources and reagents should be directed to and will be fulfilled by the lead contact, David S. Yu (dsyu@emory.edu).

Materials availability—All newly created reagents made during this study are available upon request to the lead contact.

Data and code availability—This study did not create or analyze any codes or datasets.

EXPERIMENTAL MODEL AND SUBJECT DETAILS

Cell lines—Human HEK293T (fetal), U2OS (female), and HCT116 (male) cell lines were originally purchased from the American Type Culture Collection (ATCC, Manassas, VA). U2OS-235 mCherry-LacI-FokI cell lines (female) were kindly provided by Dr. Roger Greenberg and have been described previously (Shanbhag and Greenberg, 2013). U2OS-DR-GFP cell lines were kindly provided by Dr. Jeremy Stark and have been described previously (Pierce et al., 1999). All cell lines were grown in DMEM (GIBCO) with 7.5% FBS. All cell lines were grown at 37°C under humidified conditions with 5% CO_2 and 95% air.

METHOD DETAILS

Transfections—Transfections were done on 5 million cells in 60 mm plates using Lipofectamine 2000 or 3000 (Invitrogen) and performed per the manufacturer's instructions. 5 to 10 μg of the indicated plasmids were used. Cells were split after 16 hours of incubation and allowed to recover for a further 24-48 hours post-transfection before harvest.

Immunoprecipitation—Briefly, cells were harvested and washed once with PBS. Cells were then lysed for 30 minutes on ice with CHAPS buffer (10% (vol/vol) glycerol, 150 mM NaCl, 50 mM Tris pH 7.5, 0.75% CHAPS) with the usual protease inhibitors added fresh. 1 μM TSA and 20 μM of nicotinamide were added with the usual protease inhibitors when probing for acetylation. The cells were then spun down for 15 minutes at 4°C and the resulting pellet discarded. An equal volume of minus CHAPS buffer (10% (vol/vol) glycerol, 150 mM NaCl, 50 mM Tris pH 7.5) was added to the supernatant to dilute the CHAPS concentration to 0.375%. The lysate was precleared via incubation for an hour with 30 μL of either protein G agarose beads (Invitrogen) or protein A agarose beads (Invitrogen). Protein G agarose beads were used when the IP antibody was mouse, while protein A agarose beads were used when the IP antibody was rabbit. The lysate was then added to 30 μL of preconjugated beads overnight on a rotator at 4°C. FLAG-tagged proteins were IP'd using FLAG M2 affinity beads (Sigma) while HA-tagged proteins were IP'ed using HA agarose beads (a2095; Sigma). Endogenous IPs were done with the indicated antibody. Negative controls consisted of IP with lysate using IgG rabbit or mouse for endogenous IPs and lysate not expressing tagged proteins for non-endogenous IPs. The beads were then washed three times with the 0.375% CHAPS buffer. The beads were then resuspended in 15 μL of 0.375% CHAPS buffer and 5 μL of 4× SDS before being boiled for 5 minutes at 100°C before being run on an SDS-PAGE. Immunoprecipitation experiments were each performed at least 4 times total.

DR-GFP assay—To measure efficiency of HR-mediated DSB repair, 3 million U2OS cells stably expressing a DR-GFP reporter gene, described previously (Pierce et al., 1999), were transfected with 60 nM of siRNA using Lipofectamine RNAiMax (Invitrogen) as per the manufacturer's instructions. The next day, media was removed, and cells were transfected with 5 μg I-SceI and/or 2 μg the indicated plasmid. 72 hours after transfection, cells were harvested for flow cytometry and the data analyzed to measure HR efficiency based on GFP

expression. Experiments were repeated at least three times and tested for significance using a paired one-tailed t test.

Immunoblot—Cells were harvested and washed once with PBS. Cells were then lysed for 30 minutes on ice using a 1% Nonidet P-40 (NP-40), 250 mM NaCl, 50 mM HEPES pH 7.9, 1 mM $MgCl_2$, 1 mM DTT, and 0.5 mM EDTA buffer with freshly added protease inhibitors. Samples were then resolved by SDS-PAGE and probed with the antibodies indicated in the figure. Signal detection was done with a Li-Cor Odyssey system. All western blot experiments were done at least 3 times. Quantification was done using ImageJ and statistical analysis was done by GraphPad Prism 7 using a one-sample t test.

Antibodies and reagents—The following antibodies were used: BRCA1 (ab16780, Abcam: 1/1000 for western and 1/200 for IF) and (sc-6954, Santa Cruz Biotechnology: 1/300 for western). BARD1 (A300-263A; Bethyl, 1/1000 for western), (E-11; Santa Cruz Biotechnology, 1/1000 for western), (ab226854; Abcam, 1/800 for IF), and (Antiserum 59P; a generous gift from Dr. Richard Baer we gratefully thank him for, 1/50 for IP). H2AX (s139; Cell Signaling Technology, 1/200 for IF) and (05-636 clone JB2301; MilliporeSigma, 1/4000 for IF). GAPDH (sc-47224; Santa Cruz Biotechnology, 1/1000 for western). Acetyl lysine (ICP0380; Immunechem, 1/500 for western). SIRT2 (09-843; Millipore, 1/500 for western), and (custom-made; ThermoFisher, 1/1000 for western). α-tubulin (T6074; Sigma-Aldrich, 1/1000 for western). Acetyl α-tubulin (ab179484; Abcam, 1/1000 for western). FLAG (2368S; Cell Signaling Technology, 1/1000 for western) and (sc-51590; Santa Cruz Biotechnology, 1/1000 for western). HA (H9658 clone HA-7; Sigma-Aldrich, 1/1000 for western) and (c29F4; Cell Signaling Technology, 1/1000 for western). GFP (ab290; Abcam, 1/1000 for western and 1 μL antibody per 2 mg lysate for IP) and (sc-996; Santa Cruz Biotechnology, 1/1000 for western). RAD51 (PC130; Millipore, 1:1000 for IF). IgG (10500C; Invitrogen) and (NI03; MilliporeSigma). Secondary antibodies: Cy5 (Goat anti-rabbit Alexa-Flour-647 secondary Ab) (A12244; Invitrogen, 1/1000 for IF), Alexa Fluor 488 or 555, mouse or rabbit (Invitrogen, 1/1000 for IF, 1/10000 for western). MG132 (Sigma-Aldrich; 1211877-36-9) was used at a 5 μM dose for 6 hours while AGK2 (Selleckchem; S7577) was used at a 32 μM or at the indicated concentration.

***In vitro* deacetylation assay—**To purify SIRT2-FLAG from cells, HEK293T cells were transfected with 5 μg of SIRT2-FLAG. 48 hours post-transfection, cells were lysed using an *in vitro* deacetylase buffer (180 mM KCl, 20 mM HEPES pH 7.4,1.5 mM $MgCl_2$, 0.2 mM EGTA, 20% glycerol, and 1% NP-40) supplemented with fresh protease inhibitors. A FLAG IP was performed overnight after an hour of preclearing with CL-4B Sepharose beads. After three washes with TBS buffer (50 mM Tris pH 7.5, 150 mM NaCl), the beads were resuspended in TBS buffer (50 mM Tris pH 7.5, 150 mM NaCl)where SIRT2-FLAG was eluted over the course of an hour on a cold rotator using 5 μL of FLAG peptide (Sigma) per 100 μL TBS. The supernatant was then collected and stored at −80°C for future use. To determine enzyme concentration, a sample of the supernatant was run on a western along with a BSA standard. For the deacetylation assay, HEK293T cells were transfected with the indicated plasmid. After 36 hours, cells were treated with 10 mM of nicotinamide and 0.5 μM of trichostatin A (TSA), a class I and II deacetylase inhibitor, for an additional 12 hours.

Cells were then harvested using the *in vitro* deacetylase buffer supplemented with protease inhibitors and 20 mM of nicotinamide and 1 μM of TSA. An IP was then done on the tag of the transfected plasmid. The beads were then washed three times with and resuspended in deacetylation buffer not containing nicotinamide or TSA. The beads were then split evenly between the different experimental groups. SIRT2-FLAG and the other indicated components were then added to their respective tube. The final amounts and concentrations per condition used were: ~1 μg of SIRT2-FLAG (WT or H187Y) per 24 μL of total volume, 1 μM TSA (all conditions), 25 mM nicotinamide, 625 μM of $MgCl_2$ (all conditions), and 10 mM of NAD^+ (all conditions). Tubes containing the beads and the indicated reagents were then added to a 30°C water bath where the beads were gently agitated every 15 minutes to maintain proper mixing. After 3 hours, 4× SDS was added to each sample and then run on a western blot for analysis. For BRCA1 (*in vitro* and in cells), 3 μg of the histone acetylases (HATs) p300, pCAF, and CBP were transfected with BRCA1 to increase the acetylation signal.

Immunofluorescence—For U2OS-265 mCherry-LacI-FokI cells, the cells were grown in 2 μg puromycin and 100 μg/mL hygromycin. After 72 hours of siRNA treatment and 48 hours of transfection with the indicated reagents, m-Cherry-FokI was induced for 4 hours with 1 μM of Shield-1 (Takara, 632189) and 1 μM of 4-hydroxytamoxifen (4-OHT; Sigma, H7904). For all cells, after the indicated treatment, the indicated cells were seeded on coverslips and allowed the indicated recovery time. Cells were then either permeabilized in CSK buffer with 0.5% triton-X for 5 minutes then fixed in 4% PFA for 10 minutes, or fixed in 4% PF1 for 10 minutes first and then permeabilized with 0.5% triton-X for 10 minutes in PBS buffer. Cells were blocked in PBS with 15% FBS for one hour then immunostained for one hour or overnight with the indicated primary antibodies in PBS with 15% FBS. Cells were then incubated with secondary antibody (Alexa Fluor 488 or 555 mouse or rabbit, Invitrogen) for one hour before being mounted onto slides using DAPI Fluoromount-G® (SouthernBiotech, 0100–20). The percentage of cells showing cytoplasmic BRCA1 or BARD1 localization in Figures 3A, 3C, and 3E was counted from 100 cells per replica with three replicas and significance between groups calculated using a paired one-tailed t test. In Figure S3A, the indicated number of cells had fluorescence quantified using using ImageJ. Statistical analysis between the groups was done via a two-way ANOVA using GraphPad Prism 7. In Figure S5K, cells were counted in triplicate and percentage of RAD51 localization with FokI/GFP foci was determined. Statistical analysis between the groups was done via a two-way ANOVA using GraphPad Prism 7. Most images were captured on a Zeiss Observer Z1 microscope using AxioVision Rel 4.8 software at 63x magnification. Cells in Figures S3A and S5K were visualized for using the Leica SP8 inverted confocal microscope at 63X magnification.

RT-qPCR—Briefly, cells were first lysed with TRIzol. 200 μL of chloroform was added per mL of TRIzol then set on a rocker for 15 minutes at room temperature. The samples were centrifuged for 15 minutes at 12k rpm at room temperature and the aqueous phase collected. A 1:1 volume of isopropanol was added to the aqueous phase then allowed to incubate for 2 hours on ice. The samples were again centrifuged for 15 minutes at 12k rpm to pellet the RNA. The RNA was washed once with 75% ethanol and allowed to air-dry before being

resuspended in nuclease-free water. cDNA was then created using an OligoT kit (18080–051; Invitrogen) using a C1000© Thermal Cycler (Bio-Rad). Taqman probes to each DNA sequence of interest were then used for qPCR. The probes used were: BRCA1 (TaqMan Hs01556193_m1; ThermoFisher), BARD1 (TaqMan Hs00957646_m1; ThermoFisher), and GAPDH (TaqMan Hs99999905_m1; ThermoFisher). Each experiment was done in triplicate with four internal replicates per sample. qPCR was performed on a 7500 Fast Real-Time PCR system (ThermoFisher). Results were analyzed using a paired two-tailed t test using GraphPad Prism 7.

Knock down—Knockdowns were done using RNAi Max reagent (Invitrogen) and performed per the manufacturer's instructions. Cells would be split after 24 hours of incubation and allowed to recover for a further 48 hours. The following siRNAs were used: BRCA1 (M-003461-02; Dharmacon). SIRT2-1 (D-004826-05; Dharmacon) and SIRT2-2 (s105116657; QIAGEN).

Cell cycling—24 hours after siRNA transfection, 400,000 HCT116 cells were plated on a 60 mm plate. On day 2, the 24-hour release cells were treated with 500 μM mimosine. On day 3, the mimosine was removed from the 24-hour release condition with 2x washes of PBS and media with a 1/50,000 dilution of 10 mg/mL nocodazole, while the 0-hour and 7-hour conditions were treated with 500 μM mimosine. On day 4, the 7-hour condition was released with 2x washes of PBS with 1/50,000 dilution of 10 mg/mL nocodazole, and all samples were harvested at the same time. The samples were then split into two for flow and western analysis.

Plasmids—The following plasmids were used: HA-BRCA1 is 1xMyc-3xHA-BRCA1 in the pcDNA3.1 backbone, where HA-BRCA1 C61G was made from the same plasmid by the Emory Integrated Genomics Core. GFP-BARD1 was kindly provided by Dr. Xiaochun Yu and made has been described previously (Li and Yu, 2013). BRCA1 fragments, including 167 BRCA1 and 14KR, were generously provided by Dr. Yanfen Hu and are as previously described (Lu et al., 2007). His-SIRT2 was a kind gift from Dr. Michael Tainsky's lab and has been previously described (Dryden et al., 2003). SIRT2-FLAG WT is from Dr. Eric Verdin (Addgene 13813) and H187Y is a derivative. FLAG-BARD1 WT, 1-202, Δ34-126, and BARD1 antiserum 59P were graciously provided by Dr. Richard Baer (Laufer et al., 2007; Wu et al., 1996).

QUANTIFICATION AND STATISTICAL ANALYSIS

Statistical details of each experiment can be found in the Figure Legends. The number of experimental replicates are indicated in the figure legends or outlined in the Method Details. Statistical comparisons included one- and two-way ANOVA and Student's t test as specified in the Figure Legends using Prism software (GraphPad version 7.04) or Excel. Statistical significance was set at * indicates $p < 0.05$, ** indicates $p < 0.01$, *** indicates $p < 0.005$. Data presented in graphs are mean and SD from three replicas are shown unless stated otherwise.

Supplementary Material

Refer to Web version on PubMed Central for supplementary material.

ACKNOWLEDGMENTS

We thank members of the Yu lab for their helpful discussion and technical expertise. This work was supported by the National Institute of General Medical Sciences of the National Institutes of Health (NIH) (5T32GM008367-29); the National Cancer Institute (NCI) of the NIH (F31CA225124 to E.V.M. and R01CA178999 and R01CA254403 to D.S.Y.); the U.S. Department of Defense (OC160540 to D.S.Y.); the Basser Center for BRCA (32356 to D.S.Y.); and the Winship Cancer Institute/Brenda Nease Breast Cancer Research Fund (53237 to D.S.Y.). Research reported in this publication was supported in part by the Emory Integrated Genomics Core (EIGC) Shared Resource of Winship Cancer Institute of Emory University and the NIH/NCI under award number P30CA138292. The content is solely the responsibility of the authors and does not necessarily represent the official views of the NIH.

REFERENCES

Brzovic PS, Meza J, King MC, and Klevit RE (1998). The cancer-predisposing mutation C61G disrupts homodimer formation in the NH2-terminal BRCA1 RING finger domain. J. Biol. Chem 273, 7795–7799. [PubMed: 9525870]

Brzovic PS, Meza JE, King MC, and Klevit RE (2001a). BRCA1 RING domain cancer-predisposing mutations. Structural consequences and effects on protein-protein interactions. J. Biol. Chem 276, 41399–41406. [PubMed: 11526114]

Brzovic PS, Rajagopal P, Hoyt DW, King MC, and Klevit RE (2001b). Structure of a BRCA1-BARD1 heterodimeric RING-RING complex. Nat. Struct. Biol 8, 833–837. [PubMed: 11573085]

Brzovic PS, Keeffe JR, Nishikawa H, Miyamoto K, Fox D 3rd, Fukuda M, Ohta T, and Klevit R (2003). Binding and recognition in the assembly of an active BRCA1/BARD1 ubiquitin-ligase complex. Proc. Natl. Acad. Sci. U S A 100, 5646–5651. [PubMed: 12732733]

Castilla LH, Couch FJ, Erdos MR, Hoskins KF, Calzone K, Garber JE, Boyd J, Lubin MB, Deshano ML, Brody LC, et al. (1994). Mutations in the BRCA1 gene in families with early-onset breast and ovarian cancer. Nat. Genet 8, 387–391. [PubMed: 7894491]

Chang S, and Sharan SK (2012). BRCA1 and microRNAs: emerging networks and potential therapeutic targets. Mol. Cells 34, 425–432. [PubMed: 22936386]

Choudhury AD, Xu H, and Baer R (2004). Ubiquitination and proteasomal degradation of the BRCA1 tumor suppressor is regulated during cell cycle progression. J. Biol. Chem 279, 33909–33918. [PubMed: 15166217]

Drost R, Bouwman P, Rottenberg S, Boon U, Schut E, Klarenbeek S, Klijn C, van der Heijden I, van der Gulden H, Wientjens E, et al. (2011). BRCA1 RING function is essential for tumor suppression but dispensable for therapy resistance. Cancer Cell 20, 797–809. [PubMed: 22172724]

Dryden SC, Nahhas FA, Nowak JE, Goustin AS, and Tainsky MA (2003). Role for human SIRT2 NAD-dependent deacetylase activity in control of mitotic exit in the cell cycle. Mol. Cell. Biol 23, 3173–3185. [PubMed: 12697818]

Fabbro M, Rodriguez JA, Baer R, and Henderson BR (2002). BARD1 induces BRCA1 intranuclear foci formation by increasing RING-dependent BRCA1 nuclear import and inhibiting BRCA1 nuclear export. J. Biol. Chem 277, 21315–21324. [PubMed: 11925436]

Finkel T, Deng CX, and Mostoslavsky R (2009). Recent progress in the biology and physiology of sirtuins. Nature 460, 587–591. [PubMed: 19641587]

Foulkes WD (2008). Inherited susceptibility to common cancers. N. Engl. J. Med 359, 2143–2153. [PubMed: 19005198]

Friedman LS, Ostermeyer EA, Szabo CI, Dowd P, Lynch ED, Rowell SE, and King MC (1994). Confirmation of BRCA1 by analysis of germline mutations linked to breast and ovarian cancer in ten families. Nat. Genet 8, 399–404. [PubMed: 7894493]

Guarente L (2011). Franklin H. Epstein Lecture: sirtuins, aging, and medicine. N. Engl. J. Med 364, 2235–2244. [PubMed: 21651395]

Hashizume R, Fukuda M, Maeda I, Nishikawa H, Oyake D, Yabuki Y, Ogata H, and Ohta T (2001). The RING heterodimer BRCA1-BARD1 is a ubiquitin ligase inactivated by a breast cancer-derived mutation. J. Biol. Chem 276, 14537–14540. [PubMed: 11278247]

Hatchi E, Skourti-Stathaki K, Ventz S, Pinello L, Yen A, Kamieniarz-Gdula K, Dimitrov S, Pathania S, McKinney KM, Eaton ML, et al. (2015). BRCA1 recruitment to transcriptional pause sites is required for R-loop-driven DNA damage repair. Mol. Cell 57, 636–647. [PubMed: 25699710]

Head PE, Zhang H, Bastien AJ, Koyen AE, Withers AE, Daddacha WB, Cheng X, and Yu DS (2017). Sirtuin 2 mutations in human cancers impair its function in genome maintenance. J. Biol. Chem 292, 9919–9931. [PubMed: 28461331]

Hu WL, Jin L, Xu A, Wang YF, Thorne RF, Zhang XD, and Wu M. (2018). GUARDIN is a p53-responsive long non-coding RNA that is essential for genomic stability. Nat. Cell Biol 20, 492–502. [PubMed: 29593331]

Irminger-Finger I, and Jefford CE (2006). Is there more to BARD1 than BRCA1? Nat. Rev. Cancer 6, 382–391. [PubMed: 16633366]

Jiang Q, and Greenberg RA (2015). Deciphering the BRCA1 tumor suppressor network. J. Biol. Chem 290, 17724–17732. [PubMed: 26048987]

Joukov V, Chen J, Fox EA, Green JB, and Livingston DM (2001). Functional communication between endogenous BRCA1 and its partner, BARD1, during Xenopus laevis development. Proc. Natl. Acad. Sci. U S A 98, 12078–12083. [PubMed: 11593018]

Kawai S, and Amano A (2012). BRCA1 regulates microRNA biogenesis via the DROSHA microprocessor complex. J. Cell Biol 197, 201–208. [PubMed: 22492723]

Kim HS, Vassilopoulos A, Wang RH, Lahusen T, Xiao Z, Xu X, Li C, Veenstra TD, Li B, Yu H, et al. (2011). SIRT2 maintains genome integrity and suppresses tumorigenesis through regulating APC/C activity. Cancer Cell 20, 487–499. [PubMed: 22014574]

Kim JL, Ha GH, Campo L, and Breuer EK (2018). Negative regulation of BRCA1 by transforming acidic coiled-coil protein 3 (TACC3). Biochem. Biophys. Res. Commun 496, 633–640. [PubMed: 29355525]

Kim S, Jin H, Seo HR, Lee HJ, and Lee YS (2019). Regulating BRCA1 protein stability by cathepsin S-mediated ubiquitin degradation. Cell Death Differ 26, 812–825. [PubMed: 30006610]

Kleiman FE, and Manley JL (1999). Functional interaction of BRCA1-associated BARD1 with polyadenylation factor CstF-50. Science 285, 1576–1579. [PubMed: 10477523]

Kleiman FE, and Manley JL. (2001). The BARD1-CstF-50 interaction links mRNA 3′ end formation to DNA damage and tumor suppression. Cell 104, 743–753. [PubMed: 11257228]

Kolinjivadi AM, Sannino V, de Antoni A, Técher H, Baldi G, and Costanzo V (2017). Moonlighting at replication forks—a new life for homologous recombination proteins BRCA1, BRCA2 and RAD51. FEBS Lett 591, 1083–1100. [PubMed: 28079255]

Lahusen TJ, Kim SJ, Miao K, Huang Z, Xu X, and Deng CX (2018). BRCA1 function in the intra-S checkpoint is activated by acetylation via a pCAF/SIRT1 axis. Oncogene 37, 2343–2350. [PubMed: 29440709]

Laufer M, Nandula SV, Modi AP, Wang S, Jasin M, Murty VV, Ludwig T, and Baer R (2007). Structural requirements for the BARD1 tumor suppressor in chromosomal stability and homology-directed DNA repair. J. Biol. Chem 282, 34325–34333. [PubMed: 17848578]

Lee C, Banerjee T, Gillespie J, Ceravolo A, Parvinsmith MR, Starita LM, Fields S, Toland AE, and Parvin JD (2015). Functional analysis of BARD1 missense variants in homology-directed repair of DNA double strand breaks. Hum. Mutat 36, 1205–1214. [PubMed: 26350354]

Li M, and Yu X (2013). Function of BRCA1 in the DNA damage response is mediated by ADP-ribosylation. Cancer Cell 23, 693–704. [PubMed: 23680151]

Lu Y, Amleh A, Sun J, Jin X, McCullough SD, Baer R, Ren D, Li R, and Hu Y (2007). Ubiquitination and proteasome-mediated degradation of BRCA1 and BARD1 during steroidogenesis in human ovarian granulosa cells. Mol. Endocrinol 21, 651–663. [PubMed: 17185394]

Lu Y, Li J, Cheng D, Parameswaran B, Zhang S, Jiang Z, Yew PR, Peng J, Ye Q, and Hu Y (2012). The F-box protein FBXO44 mediates BRCA1 ubiquitination and degradation. J. Biol. Chem 287, 41014–41022. [PubMed: 23086937]

Lu Q, Zhang FL, Lu DY, Shao ZM, and Li DQ (2019). USP9Xstabilizes BRCA1 and confers resistance to DNA-damaging agents in human cancer cells. Cancer Med 8, 6730–6740. [PubMed: 31512408]

Mallery DL, Vandenberg CJ, and Hiom K (2002). Activation of the E3 ligase function of the BRCA1/BARD1 complex by polyubiquitin chains. EMBO J 21, 6755–6762. [PubMed: 12485996]

Meza JE, Brzovic PS, King MC, and Klevit RE (1999). Mapping the functional domains of BRCA1. Interaction of the ring finger domains of BRCA1 and BARD1.J. Biol. Chem 274, 5659–5665. [PubMed: 10026184]

Morris JR, Keep NH, and Solomon E (2002). Identification of residues required for the interaction of BARD1 with BRCA1. J. Biol. Chem 277, 9382–9386. [PubMed: 11773071]

Moynahan ME, and Jasin M (2010). Mitotic homologous recombination maintains genomic stability and suppresses tumorigenesis. Nat. Rev. Mol. Cell Biol 11, 196–207. [PubMed: 20177395]

Moynahan ME, Chiu JW, Koller BH, and Jasin M (1999). Brca1 controls homology-directed DNA repair. Mol. Cell 4, 511–518. [PubMed: 10549283]

Moynahan ME, Cui TY, and Jasin M (2001). Homology-directed DNA repair, mitomycin-c resistance, and chromosome stability is restored with correction of a Brca1 mutation. Cancer Res 61, 4842–4850. [PubMed: 11406561]

North BJ, Marshall BL, Borra MT, Denu JM, and Verdin E (2003). The human Sir2 ortholog, SIRT2, is an NAD+-dependent tubulin deacetylase. Mol. Cell 11, 437–444. [PubMed: 12620231]

Outeiro TF, Kontopoulos E, Altmann SM, Kufareva I, Strathearn KE, Amore AM, Volk CB, Maxwell MM, Rochet JC, McLean PJ, et al. (2007). Sirtuin 2 inhibitors rescue alpha-synuclein-mediated toxicity in models of Parkinson's disease. Science 317, 516–519. [PubMed: 17588900]

Peng Y, Dai H, Wang E, Lin CC, Mo W, Peng G, and Lin SY (2015). TUSC4 functions as a tumor suppressor by regulating BRCA1 stability. Cancer Res 75, 378–386. [PubMed: 25480944]

Pierce AJ, Johnson RD, Thompson LH, and Jasin M (1999). XRCC3 promotes homology-directed repair of DNA damage in mammalian cells. Genes Dev 13, 2633–2638. [PubMed: 10541549]

Rodriguez JA, Schüchner S, Au WW, Fabbro M, and Henderson BR (2004). Nuclear-cytoplasmic shuttling of BARD1 contributes to its proapoptotic activity and is regulated by dimerization with BRCA1. Oncogene 23, 1809–1820. [PubMed: 14647430]

Roy R, Chun J, and Powell SN (2011). BRCA1 and BRCA2: different roles in a common pathway of genome protection. Nat. Rev. Cancer 12, 68–78. [PubMed: 22193408]

Ruffner H, Joazeiro CA, Hemmati D, Hunter T, and Verma IM (2001). Cancer-predisposing mutations within the RING domain of BRCA1: loss of ubiquitin protein ligase activity and protection from radiation hypersensitivity. Proc. Natl. Acad. Sci. U S A 98, 5134–5139. [PubMed: 11320250]

Saunders LR, and Verdin E (2007). Sirtuins: critical regulators at the cross-roads between cancer and aging. Oncogene 26, 5489–5504. [PubMed: 17694089]

Savage KI, Gorski JJ, Barros EM, Irwin GW, Manti L, Powell AJ, Pellagatti A, Lukashchuk N, McCance DJ, McCluggage WG, et al. (2014). Identification of a BRCA1-mRNA splicing complex required for efficient DNA repair and maintenance of genomic stability. Mol. Cell 54, 445–459. [PubMed: 24746700]

Schneider CA, Rasband WS, and Eliceiri KW (2012). NIH Image to ImageJ: 25 years of image analysis. Nat. Methods 9, 671–675. [PubMed: 22930834]

Schlacher K, Wu H, and Jasin M (2012). A distinct replication fork protection pathway connects Fanconi anemia tumor suppressors to RAD51-BRCA1/2. Cancer Cell 22, 106–116. [PubMed: 22789542]

Scully R, Chen J, Ochs RL, Keegan K, Hoekstra M, Feunteun J, and Livingston DM (1997). Dynamic changes of BRCA1 subnuclear location and phosphorylation state are initiated by DNA damage. Cell 90, 425–435. [PubMed: 9267023]

Serrano L, Martínez-Redondo P, Marazuela-Duque A, Vazquez BN, Dooley SJ, Voigt P, Beck DB, Kane-Goldsmith N, Tong Q, Rabanal RM, et al. (2013). The tumor suppressor SirT2 regulates cell cycle progression and genome stability by modulating the mitotic deposition of H4K20 methylation. Genes Dev 27, 639–653. [PubMed: 23468428]

Shakya R, Szabolcs M, McCarthy E, Ospina E, Basso K, Nandula S, Murty V, Baer R, and Ludwig T (2008). The basal-like mammary carcinomas induced by Brca1 or Bard1 inactivation implicate the

BRCA1/BARD1 heterodimer in tumor suppression. Proc. Natl. Acad. Sci. U S A 105, 7040–7045. [PubMed: 18443292]

Shanbhag NM, and Greenberg RA (2013). The dynamics of DNA damage repair and transcription. Methods Mol. Biol 1042, 227–235. [PubMed: 23980011]

Shanbhag NM, Rafalska-Metcalf IU, Balane-Bolivar C, Janicki SM, and Greenberg RA (2010). ATM-dependent chromatin changes silence transcription in cis to DNA double-strand breaks. Cell 141, 970–981. [PubMed: 20550933]

Silver DP, and Livingston DM (2012). Mechanisms of BRCA1 tumor suppression. Cancer Discov 2, 679–684. [PubMed: 22843421]

Snouwaert JN, Gowen LC, Latour AM, Mohn AR, Xiao A, DiBiase L, and Koller BH (1999). BRCA1 deficient embryonic stem cells display a decreased homologous recombination frequency and an increased frequency of non-homologous recombination that is corrected by expression of a brca1 transgene. Oncogene 18, 7900–7907. [PubMed: 10630642]

Song L, and Rape M (2010). Regulated degradation of spindle assembly factors by the anaphase-promoting complex. Mol. Cell 38, 369–382. [PubMed: 20471943]

Tarsounas M, and Sung P. (2020). The antitumorigenic roles of BRCA1-BARD1 in DNA repair and replication. Nat. Rev. Mol. Cell Biol 21, 284–299. [PubMed: 32094664]

Ueki T, Park JH, Nishidate T, Kijima K, Hirata K, Nakamura Y, and Katagiri T (2009). Ubiquitination and downregulation of BRCA1 by ubiquitin-conjugating enzyme E2T overexpression in human breast cancer cells. Cancer Res 69, 8752–8760. [PubMed: 19887602]

Venkitaraman AR (2014). Cancer suppression by the chromosome custodians, BRCA1 and BRCA2. Science 343, 1470–1475. [PubMed: 24675954]

Wang X, Lu G, Li L, Yi J, Yan K, Wang Y, Zhu B, Kuang J, Lin M, Zhang S, and Shao G (2014). HUWE1 interacts with BRCA1 and promotes its degradation in the ubiquitin-proteasome pathway. Biochem. Biophys. Res. Commun 444, 549–554. [PubMed: 24472556]

Wu LC, Wang ZW, Tsan JT, Spillman MA, Phung A, Xu XL, Yang MC, Hwang LY, Bowcock AM, and Baer R (1996). Identification of a RING protein that can interact in vivo with the BRCA1 gene product. Nat. Genet 14, 430–440. [PubMed: 8944023]

Wu W, Sato K, Koike A, Nishikawa H, Koizumi H, Venkitaraman AR, and Ohta T (2010). HERC2 is an E3 ligase that targets BRCA1 for degradation. Cancer Res 70, 6384–6392. [PubMed: 20631078]

Xia Y, Pao GM, Chen HW, Verma IM, and Hunter T (2003). Enhancement of BRCA1 E3 ubiquitin ligase activity through direct interaction with the BARD1 protein. J. Biol. Chem 278, 5255–5263. [PubMed: 12431996]

Xu X, Weaver Z, Linke SP, Li C, Gotay J, Wang XW, Harris CC, Ried T, and Deng CX (1999). Centrosome amplification and a defective G2-M cell cycle checkpoint induce genetic instability in BRCA1 exon 11 isoform-deficient cells. Mol. Cell 3, 389–395. [PubMed: 10198641]

Xu B, Kim St, and Kastan MB. (2001). Involvement of Brca1 in S-phase and G(2)-phase checkpoints after ionizing irradiation. Mol. Cell. Biol 21, 3445–3450. [PubMed: 11313470]

Yarden RI, Pardo-Reoyo S, Sgagias M, Cowan KH, and Brody LC (2002). BRCA1 regulates the G2/M checkpoint by activating Chk1 kinase upon DNA damage. Nat. Genet 30, 285–289. [PubMed: 11836499]

Zhang H, Park SH, Pantazides BG, Karpiuk O, Warren MD, Hardy CW, Duong DM, Park SJ, Kim HS, Vassilopoulos A, et al. (2013). SIRT2 directs the replication stress response through CDK9 deacetylation. Proc. Natl. Acad. Sci. U S A 110, 13546–13551. [PubMed: 23898190]

Zhang H, Head PE, Daddacha W, Park SH, Li X, Pan Y, Madden MZ, Duong DM, Xie M, Yu B, et al. (2016a). ATRIP deacetylation by SIRT2 drives ATR checkpoint activation by promoting binding to RPA-ssDNA. Cell Rep 14, 1435–1447. [PubMed: 26854234]

Zhang H, Head PE, and Yu DS (2016b). SIRT2 orchestrates the DNA damage response. Cell Cycle 15, 2089–2090. [PubMed: 27153288]

Zhang M, Du W, Acklin S, Jin S, and Xia F (2020). SIRT2 protects peripheral neurons from cisplatin-induced injury by enhancing nucleotide excision repair. J. Clin. Invest 130, 2953–2965. [PubMed: 32134743]

Highlights

- The SIRT2 sirtuin deacetylase binds and deacetylates the BRCA1-BARD1 complex
- BARD1 RING domain deacetylation by SIRT2 promotes BRCA1-BARD1 heterodimerization
- SIRT2 promotes BRCA1-BARD1 stability, nuclear retention, and localization
- BARD1 deacetylation by SIRT2 promotes homologous recombination repair

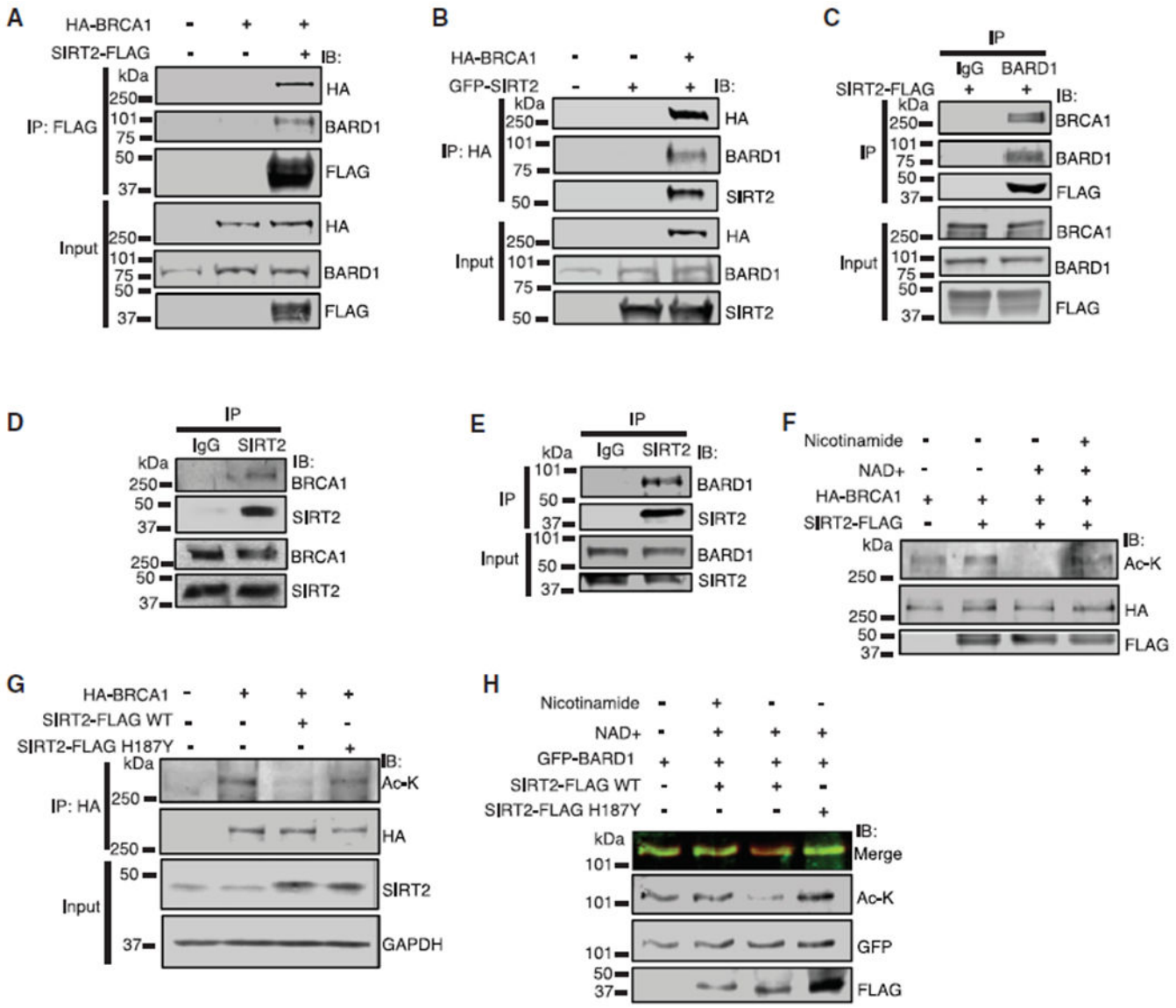

Figure 1. SIRT2 interacts with and deacetylates the BRCA1-BARD1 complex

(A) Immunoprecipitation (IP) of SIRT2-FLAG pulls down HA-BRCA1 and endogenous BARD1 in HEK293T cells.

(B) IP of HA-BRCA1 pulls down GFP-SIRT2 and endogenous BARD1 in HEK293T cells.

(C) IP of endogenous BARD1 pulls down SIRT2-FLAG and endogenous BRCA1 in HEK293T cells.

(D) Endogenous SIRT2 IP in HeLa cells pulls down endogenous BRCA1.

(E) Endogenous SIRT2 IP in HCT116 cells pulls down endogenous BARD1.

(F) SIRT2-FLAG deacetylates HA-BRCA1 *in vitro*. NAD^+ is a SIRT2 cofactor and nicotinamide inhibits class III deacetylases, including SIRT2.

(G) SIRT2-FLAG WT but not H187Y decreases HA-BRCA1 acetylation in cells.

(H) SIRT2-FLAG WT but not H187Y deacetylates GFP-BARD1 *in vitro*. Merge indicates the overlay of Ac-K (green) and GFP (red).

For (F)–(H), Ac-K indicates acetylated-lysine.
See also Figure S1.

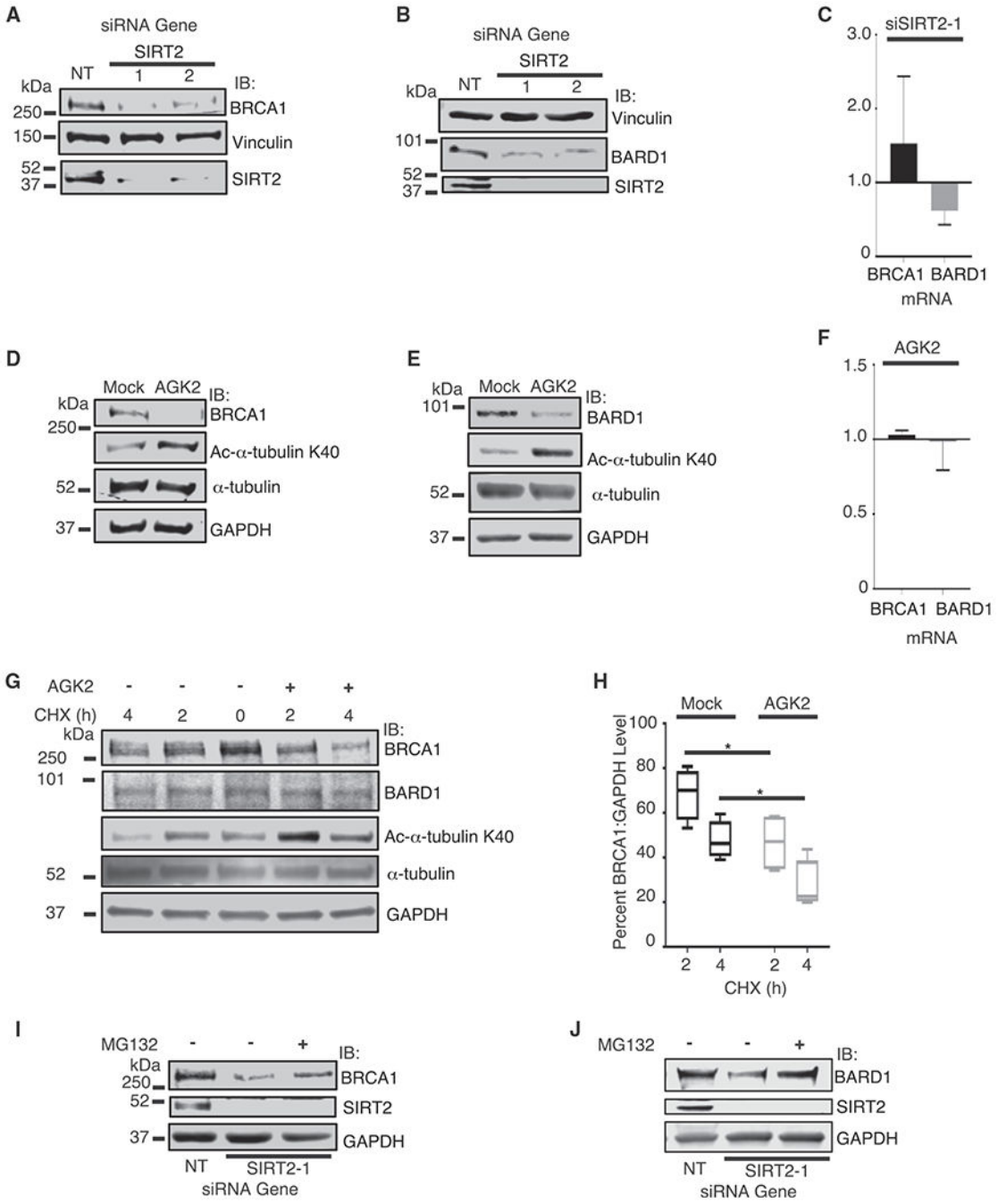

Figure 2. SIRT2 deacetylase activity promotes BRCA1-BARD1 stability

(A–C) SIRT2 knockdown decreases BRCA1 and BARD1 protein levels but does not significantly change mRNA levels in HCT116 cells.

(D–F) AGK2 treatment for 24 h decreases BRCA1 and BARD1 protein levels but shows no significant change in mRNA levels in HCT116 cells.

(G and H) HEK293T cells were treated with cycloheximide with or without AGK2 for 0, 2, or 4 h. AGK2 increases the rate of BRCA1 degradation in HEK293T cells compared with a control. Mean and SD from four independent replicas are shown.

(I) Treatment with MG132 for 6 h alleviates BRCA1 levels after SIRT2 knockdown in HCT116 cells.
(J) Treatment with MG132 for 6 h alleviates BARD1 levels after SIRT2 knockdown in HCT116 cells.
For (C) and (F), mean and SD from three independent replicas are shown. For (D) and (E), acetylated α-tubulin acts as a positive control for AGK2 treatment. *$p < 0.05$.
See also Figure S2.

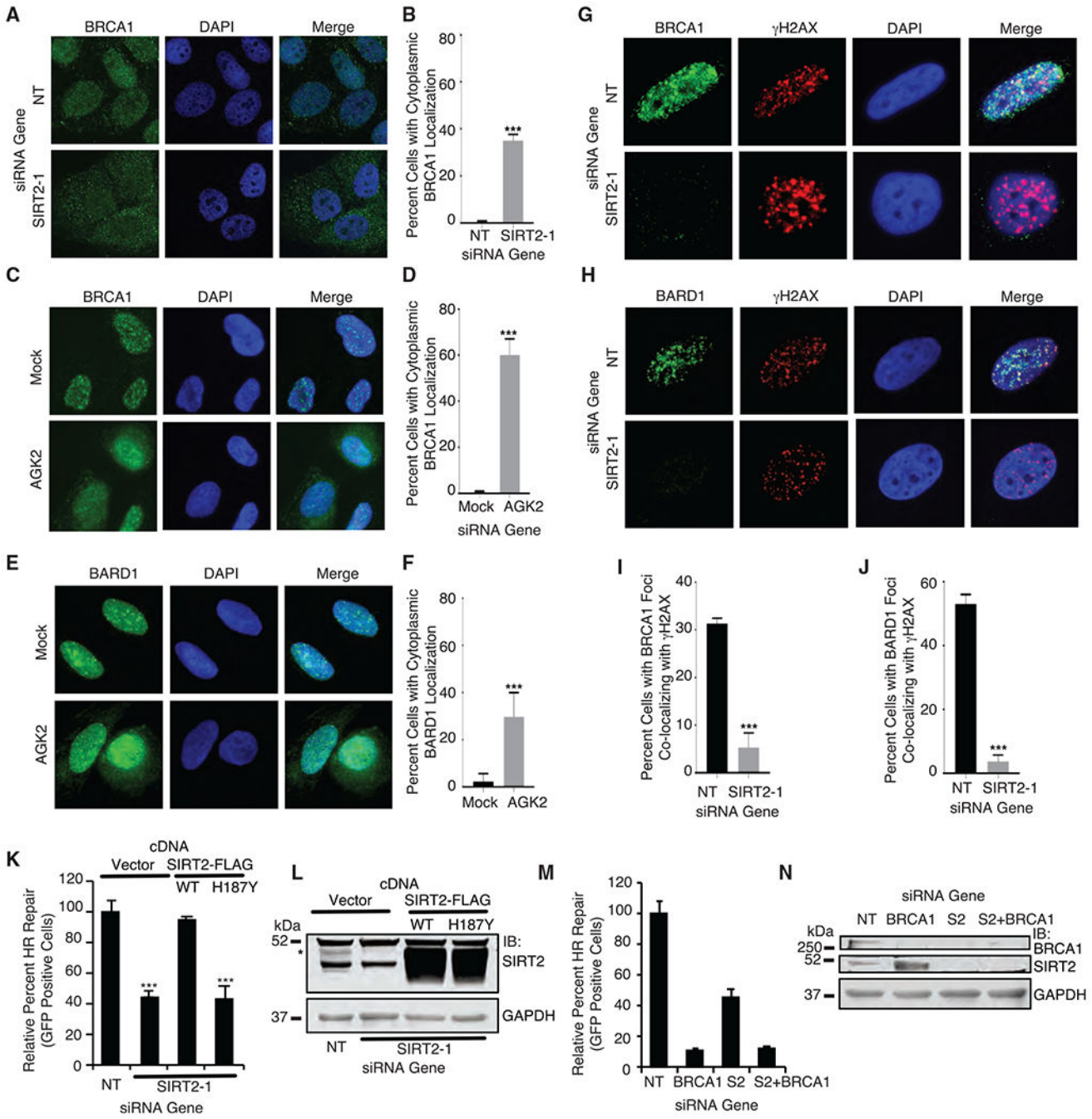

Figure 3. SIRT2 deacetylase activity promotes BRCA1-BARD1 nuclear retention, localization to DNA damage sites, and homologous recombination

(A–D) SIRT2 knockdown or inhibition with 10 μM AGK2 for 4 h in U2OS cells significantly increases cytoplasmic BRCA1.

(E and F) SIRT2 inhibition with 10 μM AGK2 for 4 h in U2OS cells significantly increases the amount of cytoplasmic BARD1.

(G–J) BRCA1 and BARD1 co-localization with γH2AX foci 4 h after 10 Gy of IR is significantly impaired in U2OS cells after SIRT2 knockdown.

(K and L) DR-GFP assay in U2OS cells showing that SIRT2 knockdown impairs HR, which can be rescued by small interfering RNA (siRNA)-resistant SIRT2-FLAG WT but not H187Y. Asterisk indicates where SIRT2 runs.

(M and N) DR-GFP assay in U2OS cells indicating that combined SIRT2 and BRCA1 knockdown does not further impair HR compared with knockdown of SIRT2 or BRCA1 alone.

For the above, mean and SD from three independent replicas are shown. ***$p < 0.005$. See also Figure S3.

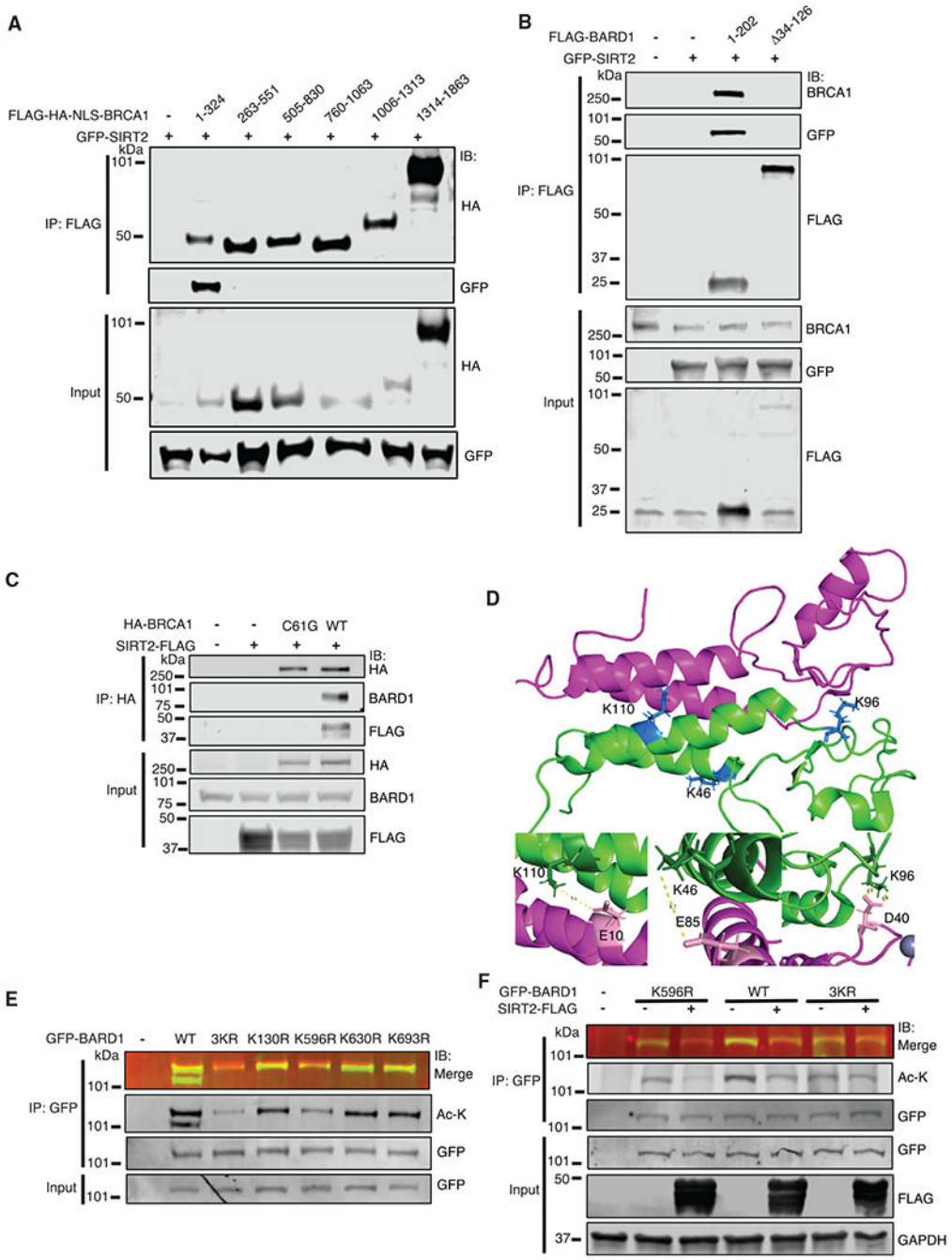

Figure 4. SIRT2 deacetylates BARD1 RING domain

(A) IP of BRCA1 fragments spanning FL BRCA1 indicates that GFP-SIRT2 pulls down BRCA1 (1–324) in HEK293T cells.

(B) IP of BARD1 fragments indicates that GFP-SIRT2 pulls down the N terminus of BARD1 (1–202), but not with BARD1 missing the RING domain (Δ34-126) in HEK293T cells.

(C) IP of HA-BRCA1 WT and C61G indicates that SIRT2-FLAG only pulls down HA-BRCA1 WT in HEK293T cells.

(D) Structure of the BRCA1-BARD1 RING domain heterodimer, indicating potential charged interactions between BARD1 K46, K96, and K110 with corresponding BRCA1 residues. BARD1 K96 is ~2.2 Å from BRCA1 D40, which may indicate a salt bridge interaction. BARD1 K110 is in close proximity, ~5.1 Å, to BRCA1 E10. BARD1 K46 is ~5.7 Å from BRCA1 E85.

(E) GFP-BARD1 WT is acetylated in cells and mutation of lysines K46, K96, and K110 to arginines (3KR) and K596 but not K130, K630, and K693 to arginines significantly decreases acetylation in HEK293T cells.

(F) SIRT2-FLAG decreases GFP-BARD1 WT and K596R but not 3KR acetylation in HEK293T cells.

For (E) and (F), merge indicates overlay of Ac-K (green) and GFP (red).

See also Figure S4.

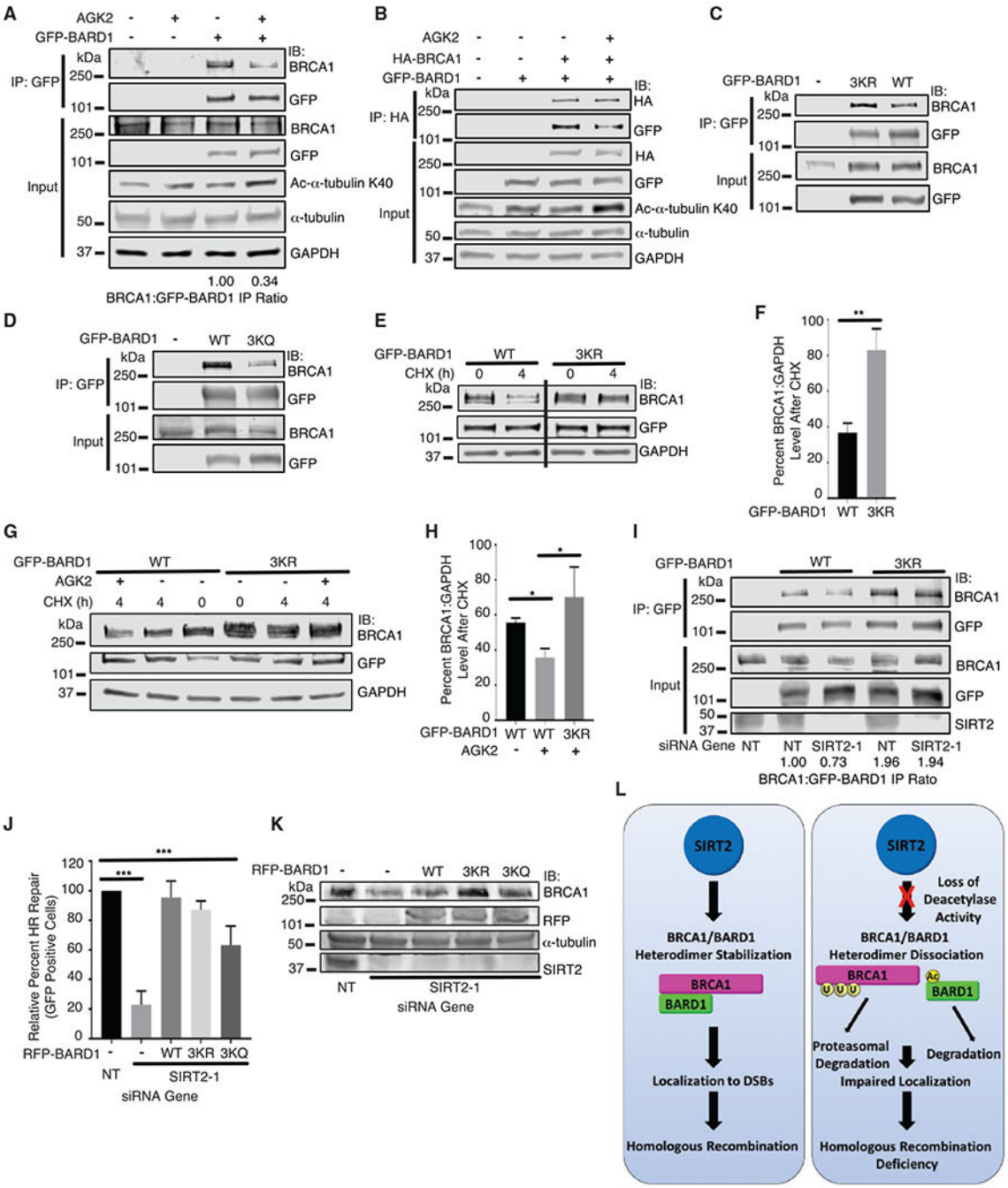

Figure 5. BARD1 RING domain deacetylation by SIRT2 promotes BRCA1-BARD1 heterodimerization

(A) coIP of GFP-BARD1 before and after 4 h of AGK2 treatment shows decreased interaction with endogenous BRCA1 in HEK293T cells.

(B) coIP of HA-BRCA1 after 4 h of AGK2 treatment shows decreased interaction with GFP-BARD1 in HEK293 T cells.

(C and D) coIP of GFP-BARD1 3KR and 3KQ show respectively increased and decreased pull-down of endogenous BRCA1 compared with GFP-BARD1 WT in HEK293T cells.

(E–H) GFP-BARD1 3KR stabilizes endogenous BRCA1 after 4 h of cycloheximide with or without AGK2 for 0 or 4 h in HEK293T cells.

(I) SIRT2 knockdown decreases the interaction between endogenous BRCA1 and GFP-BARD1 WT but not 3KR in HEK293T cells.

(J and K) DR-GFP assay showing that RFP-BARD1 WT and 3KR but not 3KQ restore the HR impairment of SIRT2 depletion to near control levels in U2OS cells.

(L) Model showing BARD1 RING domain deacetylation by SIRT2 promoting BRCA1-BARD1 heterodimerization, thereby facilitating stability, localization, and function in HR.

For the above, mean and SD from three independent replicas are shown. *$p < 0.05$, **$p < 0.01$, and ***$p < 0.005$.

See also Figure S5.

KEY RESOURCES TABLE

REAGENT or RESOURCE	SOURCE	IDENTIFIER
Antibodies		
Mouse monoclonal anti-BRCA1	Abcam	Cat# ab16780; RRID: AB_2259338
Rabbit polyclonal anti-BARD1	Bethyl	Cat# A300-263A; RRID: AB_2061250
Rabbit polyclonal anti-SIRT2	ThermoFisher custom made; This paper	N/A
Chemicals, peptides, and recombinant proteins		
AGK2	Selleckchem	Cat#S7577
MG132	Sigma-Aldrich	Cat#1211877-36-9
Critical commercial assays		
SuperScript III First-Strand Synthesis System	Invitrogen	Cat#18080-051
Experimental models: Cell lines		
Human: HEK293T	ATCC	CRL-3216
Human: HCT116	ATCC	CCL-247
Human: U2OS-265 mCherry-LacI-FokI	Laboratory of Roger Greenberg (Shanbhag and Greenberg, 2013)	N/A
Human: U2OS DR-GFP	Laboratory of Jeremy Stark (Pierce et al., 1999)	N/A
Recombinant DNA		
GFP-BARD1	Laboratory of Xiaochun Yu (Li and Yu, 2013)	N/A
FLAG-BARD1 WT, 1-202, Δ34-126	Laboratory of Richard Baer (Laufer et al., 2007)	N/A
SIRT2-FLAG	Laboratory of Eric Verdin	Addgene 13813
1xMyc-3xHA-BRCA1 pcDNA3.1	Scully et al., 1997	N/A
GFP-BARD1 3KR and 3KQ	This paper	N/A
BRCA1 Fragments	Laboratory of Yanfen Hu (Lu et al., 2007)	N/A
Software and algorithms		
GraphPad Prism 7	GraphPad Software	https://www.graphpad.com/
ImageJ	Schneider et al., 2012	https://imagej.nih.gov/ij/
FlowJo	FlowJo, LLC, BD Biosciences	https://www.flowjo.com/solutions/flowjo
Other		
Human: SIRT2-1 siRNA	Dharmacon	Cat#D-004826-05
Human: SIRT2-2 siRNA	QIAGEN	Cat#s105116657
Human: BRCA1 siRNA	Dharmacon	Cat#M-003461-02